Proc. Natl. Acad. Sci. USA
Vol. 91, pp. 9651–9654, September 1994
Genetics

P-type ATPase from the cyanobacterium *Synechococcus* 7942 related to the human Menkes and Wilson disease gene products

LE T. PHUNG*, GHADA AJLANI†‡, AND ROBERT HASELKORN*†

Departments of *Biochemistry and Molecular Biology and †Molecular Genetics and Cell Biology, University of Chicago, 920 East 58th Street, Chicago, IL 60637

Contributed by Robert Haselkorn, June 21, 1994

ABSTRACT **DNA encoding a P-type ATPase was cloned from the cyanobacterium *Synechococcus* 7942. The cloned *ctaA* gene encodes a 790-amino acid polypeptide related to the CopA Cu^{2+}-uptake ATPase of *Enterococcus hirae*, to other known P-type ATPases, and to the candidate gene products for the human diseases of copper metabolism, Menkes disease and Wilson disease. Disruption of the single chromosomal gene in *Synechococcus* 7942 by insertion of an antibiotic-resistance cassette results in a mutant cell line with increased tolerance to Cu^{2+} compared with the wild type.**

P-type ATPases are a large family of enzymes so named because of a phospho-aspartate intermediate in the ATP-driven cation transport cycle (1–3). They are found in prokaryotes as well as lower eukaryotes, plants, and animals. The most familiar P-type ATPases are the Ca^{2+}-ATPase of the muscle sarcoplasmic reticulum and the Na^+/K^+-exchange ATPase of animal cell membranes (3). A wide range of differing cation specificities has been demonstrated for P-type ATPases of prokaryotes (4). All known P-type ATPases have several regions of conserved amino acid sequences (5) including a heptapeptide with an aspartate residue that is phosphorylated and dephosphorylated during the ATPase/transport cycle (1–3). All of these membrane ATPases transport cations, but the specific cation (H^+, Na^+, K^+, Ca^{2+}, Mg^{2+}, Cd^{2+}, or Cu^{2+}) and the direction of transport (inward, outward, or cation-for-cation exchange) differ from one to another. A Cys-Pro-Cys sequence is found in the proposed membrane channel region of all bacterial P-type ATPases (4), except for the *Escherichia coli* KdpB K^+-ATPase (6, 7).

The number of identified P-type ATPases is growing rapidly. In the course of cloning other genes from *Synechococcus* 7942, we found one that appears to encode a P-type ATPase. During the preparation of this paper three other cyanobacterial P-type ATPase sequences were published (8, 9). The first of these new reports concerns two genes for P-type ATPases from the same *Synechococcus* strain used in this study (8). However, the sequences of these genes differ significantly from the one we describe here. In addition, biochemical evidence indicates that the *Synechococcus* plasma membrane contains a P-type ATPase (10).

We report the complete sequence of the DNA and the predicted gene product,§ as well as phenotypic analysis of a mutant strain of *Synechococcus* 7942 in which the gene, named here *ctaA* (Cu^{2+} transport ATPase), was inactivated. CtaA appears to be involved in Cu^{2+} transport into the cells. Although supporting data are often unavailable, it is likely that all or most prokaryotic cells have essential copper enzymes involved in electron transfer and therefore require Cu^{2+} transport systems (11).

The publication costs of this article were defrayed in part by page charge payment. This article must therefore be hereby marked "*advertisement*" in accordance with 18 U.S.C. §1734 solely to indicate this fact.

MATERIALS AND METHODS

Strains and Growth Conditions. Wild-type *Synechococcus* 7942 was grown in a modified liquid BG11 medium (12) without $Na_2SiO_3 \cdot 9H_2O$. Small cultures were grown with constant agitation in a 30°C incubator (with 2% CO_2/98% air) under white fluorescent light [about 30 $\mu E \cdot m^{-2} \cdot s^{-1}$; 1 μE (microeinstein) = 1 μmol of photons]. Large cultures were bubbled with 2% CO_2/98% air. Insertion-mutant strain K10, carrying a kanamycin-resistance cassette from pUC4K (Pharmacia), was selected on plates containing kanamycin at 50 μg/ml. For selective growth of *E. coli* strain DH5α (GIBCO/BRL) carrying antibiotic-resistance plasmids, ampicillin at 100 μg/ml or tetracycline 12 μg/ml was used.

Cloning and Sequence Determination. Standard molecular genetic techniques, including DNA isolation, restriction nuclease digestion and ligation, and Southern and Northern blotting, were as described by Sambrook *et al.* (13). Genomic DNA was prepared from cells of *Synechococcus* 7942 according to Brusslan (14). RNA isolation was as described by Schaefer and Golden (15). A fragment containing part of the *ctaA* gene was isolated from a two-step size-fractionated *Synechococcus* DNA library. *Synechococcus* genomic DNA was first digested with *Bam*HI and the restriction fragments were separated by electrophoresis in an agarose gel. Fragments of 3–6 kb were isolated and digested with *Hin*dIII. Fragments of 2–3 kb were isolated, cloned into plasmid pBR322, and transformed into *E. coli* strain DH5α. Clone pLP180 (containing a 2.6-kb *Hin*dIII–*Bam*HI fragment) was identified by screening individual plasmid DNAs with an *E. coli fabE* (16) fragment as probe. A 320-bp *Pst* I–*Bam*HI fragment was isolated from the *Hin*dIII–*Bam*HI insert of pLP180 and used as probe to screen a library of wild-type *Synechococcus* genomic DNA in the cosmid vector pWB79 (prepared by J. Brusslan, University of Chicago). A 7-kb *Hin*dIII fragment was identified and smaller restriction nuclease fragments from it were subcloned into pUC18 and pBluescript vectors (Stratagene).

Subclones for sequencing were generated either by nested deletion using the Erase-a-base kit (Promega) or by digesting the original clones with appropriate restriction nucleases and religating. Sequencing was done on both strands by the dideoxy chain-termination method with Sequenase version 2.0 (United States Biochemical) with either M13 universal and reverse primers or synthetic oligonucleotide primers. Fig. 1 summarizes the physical map of the 7-kb *Hin*dIII fragment and the 4.5-kb *Hin*dIII–*Eco*RV region within it that was sequenced completely on both strands.

Insertional Inactivation of the *ctaA* Gene. The kanamycin-resistance cassette from pUC4K was inserted between the *Bgl* II and *Pst* I sites of pLP1.5 (a pUC18-derived plasmid

‡Present address: Centre de Génétique Moléculaire, Bat. 24, Centre National de la Recherche Scientifique, F-91198 Gif-sur-Yvette, France.

§The sequence reported in this paper has been deposited in the GenBank data base (accession no. U04356).

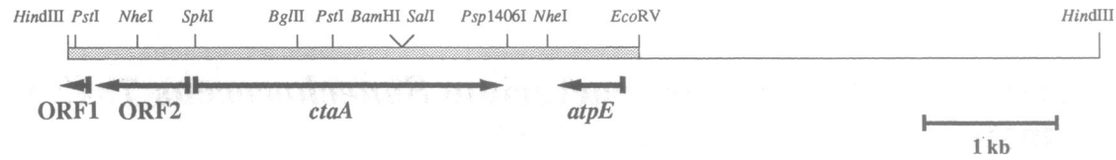

FIG. 1. Physical map of part of a 7-kb *Hin*dIII fragment of *Synechococcus* 7942 DNA carrying the *ctaA* gene. Stippled box indicates the 4.5-kb *Hin*dIII–*Eco*RV region sequenced in this work. Arrows identify the locations and orientation of genes and open reading frames (ORF1 and ORF2).

carrying a 1.5-kb *Sph* I–*Bam*HI fragment of *Synechococcus* DNA; see Fig. 1). The resulting plasmid, pLG1.5, was used to transform wild-type *Synechococcus* 7942, selecting for kanamycin-resistant (Km^r) transformants. Individual transformants were picked and grown in liquid medium containing the appropriate antibiotic. Interruption of the *ctaA* gene by insertion of the gene cassette was confirmed by Southern hybridization using the purified cassette and the 1.5-kb *Sph* I–*Bam*HI fragment as probes (data not shown). One transformant, strain K10 (Km^r), was chosen for further characterization.

Construction of Sequence Homology Trees. The trees in Fig. 4 were constructed by using the computer programs of Feng and Doolittle (17). For Fig. 4*A*, 33 amino acids from the putative metal-binding motifs were compared with one another. For Fig. 4*B*, entire amino acid sequences were used in all cases except the Menkes and Wilson disease gene products, where only the last 900 amino acids from the Menkes sequence and the last 895 amino acids from the Wilson sequence were used for comparison.

RESULTS

Cloning. The gene for the *Synechococcus* ATPase was cloned while searching for a different gene, that for the biotin-carboxyl carrier protein (BCCP), with a fragment of the *fabE* gene from *E. coli* (16) as probe. As was subsequently clarified by DNA sequencing, the *Synechococcus ctaA* fragment and the *E. coli* probe contain a perfect match of 17 nucleotides, AGCGCCAGCAGCAGCGG, a coincidence for which we lack an explanation. When the gene for BCCP from *Synechococcus* 7942 was later cloned and sequenced (L.T.P. and R.H., unpublished work), it became clear that the *Synechococcus* and *E. coli fabE* sequences are sufficiently dissimilar to preclude use of the *E. coli* gene to identify the cyanobacterial gene.

The DNA sequence of one end (see below) of the initially cloned 2.6-kb *Hin*dIII–*Sal* I fragment (Fig. 1) showed a perfect 51-nucleotide match with a sequence determined by Cozens and Walker (18) for a fragment of a gene encoding an undefined P-type ATPase, downstream and in the opposite orientation from genes for subunits β and ε of the F_1F_0 ATPase of photophosphorylation and oxidative phosphorylation from the related cyanobacterial strain *Synechococcus* 6301. We then cloned the remainder of the *Synechococcus* 7942 gene and determined its sequence and function.

Sequence Analysis. The 2.4-kb *Sph* I–*Psp*1406I region (Fig. 1) from a 4.5-kb *Hin*dIII–*Eco*RV fragment including the entire open reading frame of 2370 bp capable of encoding a 790-amino acid P-type ATPase was sequenced completely on both strands. Upstream by 833 bp from the ATPase reading frame is a 216-bp open reading frame in the opposite orientation (ORF1), potentially encoding a 72-amino acid polypeptide that is 50% identical in sequence to the N-terminal portion of the VapA protein (19) of *Dichelobacter nodosus*, the causative agent of sheep foot rot. Although thought to be in a region of *v*irulence *a*ssociated *p*roteins (hence *vap*) in *D. nodosus*, there is no evidence for a function of this protein in either *D. nodosus* or cyanobacteria. Between the *ctaA* gene and ORF1 is a 624-bp open reading frame (ORF2) in the same orientation as ORF1. The potential translation product of ORF2, however, is not sufficiently similar in sequence to anything in the available libraries to allow us to guess its function. Downstream by 394 bp from the TGA stop codon of the *ctaA* gene (Fig. 1) is the 3′ end of the *atpE* gene (encoding the ε subunit of the F_1F_0 ATPase) that was initially sequenced by Cozens and Walker (18). Since *Synechococcus* 7942 and *Synechococcus* 6301 are closely related (20), it is not surprising to find identical sequence in the *Sal* I–*Eco*RV region sequenced from both strains.

Growth of Mutant K10. In order to understand the physiological function of CtaA, mutant K10 was constructed by replacing a 400-bp *Bgl* II–*Pst* I fragment of the *ctaA* gene with a kanamycin-resistance gene cassette. Southern blot analysis (data not shown) confirmed that the cassette was inserted in the *ctaA* gene in the K10 strain. No difference in growth rate compared to the wild-type strain was observed when K10 was grown in the modified liquid BG11 medium described above (Fig. 2; circles). The wild-type and mutant strains were also grown in media supplemented with various cations (Zn^{2+}, Cd^{2+}, Cu^{2+}, Mg^{2+}, Co^{2+}, Ni^{2+}, Ag^{+}). The K10 strain was able to grow at a Cu^{2+} concentration (10 μM) that inhibited wild-type cell growth (Fig. 2, triangles). At 10 μM Cu^{2+}, wild type cells lost pigment and bleached over 3 days. The K10 cells remained green and grew after a 2-day lag. Disruption of the *ctaA* gene therefore rendered the cells more tolerant to Cu^{2+} than the wild-type cells. The other cations tested did not affect the growth of the K10 strain distinguishably from that of the wild-type strain.

DISCUSSION

The presumed amino acid translation product of the *ctaA* gene shows several conserved regions common to all P-type ATPases. Four regions with ascribed biochemical functions that are common to all P-type ATPases are shown in Fig. 3 *A–D*. Fig. 3*A* displays the "phosphatase" region (5) containing the conserved tripeptide Thr-Gly-Glu, thought to function

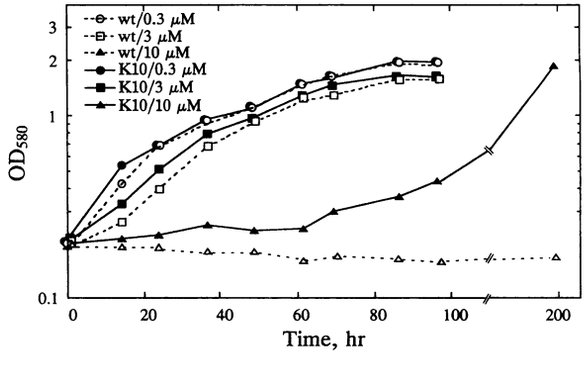

FIG. 2. Growth of wild-type and mutant *Synechococcus* 7942 in media with various Cu^{2+} concentrations. Growth was monitored by measuring optical density at 580 nm. Open symbols, wild type (wt); closed symbols, mutant K10; circles, modified liquid BG11 medium containing 0.3 μM $CuSO_4$; squares, medium containing 3 μM $CuSO_4$; triangles, medium containing 10 μM $CuSO_4$.

A. Phosphatase Region

CtaA	267	GDYVQVLPGDRIPVDGCIVAGQST-LDTAMLTGEPLPQPCQVGD	309
PacS	257	EDWVRVRPGEKVPVDGEVIDGRST-VDESMVTGESLPVQKQVGD	299
Menkes	845	GDIIKVVPGGKFPVDGRVIEGHSM-VDESLITGEAMPVAKKPGS	787
CopA	248	DDILVIRPGEQVPTDGRIIAGTSA-LDESMLTGESVPVEKKEKD	290
CopB	264	GDRLIVRAGDKMPTDGTIDKGHTI-VDESAVTGESKGVKKQVGD	306
CadA	237	GDIMIVKPGEKIAMDGIIVNGLSA-VNQAAITGESVPVSKAVDD	279
KdpB	129	GDIVLVEAGDIIPCDGEVIEGGAS-VDESAITGESAPVIRESGG	169
Pma1	153	GDIVSLASGDKVPADLRLLKVRNLQVDESALTGEAVPVEK-AVE	195
PacL	156	GDLILLEAGDQVPADARLVESANLQVKESALTGEAEAVQKLADQ	199

B. Ion Transduction Region

CtaA	425	ISVLVVACPCALGLATPTAILVATGLAAEQGILVRGGDVLE	465
PacS	383	VGVMIIACPCALGLATPTSIMVGTGKGAEYGILIKSAESLE	423
Menkes	993	ITVLCIACPCSLGLATPTAVMVGTGVGAQNGILIKGGEPLE	1033
CopA	374	VSVLVIACPCALGLATPTAIMVGTGVGAHNGILIKGGEALE	414
CopB	389	VTVFIIACPHALGLAIPLVVARSTSIAAKNGLLLKNRNAME	429
CadA	364	LAVLVVGCPCALVISTPISIVSAIGNAAKKGVLVKGGVYLE	404
KdpB	256	VALLVCLIPTTIGGLLSASAVAGMSRMLGANVIATSGRAVE	296
Pma1	292	VALAVSGIPEGLPAVVTVTLAIGVNRMAKRNAIIRKLPAVE	332
PacL	296	LSMAVAIVPEGLPAVITVALAIGTQRMVQRESLIRRLPAVE	336

C. Phosphorylation Site

CtaA	475	FDKTGTLTQGQFEL	488
PacS	433	LDKTGTLTQGQPSV	446
Menkes	1043	FDKTGTITHGTPVV	1056
CopA	424	LDKTGTITQGRPEV	437
CopB	439	LDKTGTLTQGKFTV	452
CadA	414	FDKTGTLTKGVPVV	427
KdpB	306	LDKTGTITLGNRQA	319
Pma1	342	SDKTGTLTENQMTV	356
PacL	348	SDKTGTLTQNKMVV	362

D. Hinge Region and ATP-Binding Domain

CtaA	657	LQSQGDAVAMIGDGINDAPALATAAVGISLA-AGSDIAQDSAGLLLS	702
PacS	622	LQSRGQVVAMVGDGINDAPALAQADVGIAIG-TGTDVAIAASDITLI	667
Menkes	1289	LQEEGKRVAMVGDGINDSPALAMANVGIAIG-TGTDVAIEAADVVLI	1334
CopA	609	LQKAGKKVGMVGDGINDAPALRLADVGIAMG-SGTDIAMETADVTLM	654
CopB	626	YLDQGKKVIMVGDGINDAPSLARATIGMAIG-AGTDIAIDSADVVLT	671
CadA	608	MQSEYDNVAMIGDGVNDAPALAASTVGIAMGGAGTDTAIETADIALM	654
KdpB	506	YQAEGRLVAMTGDGTNDAPALAQADVAVAMN-SGTQAAKEAGNMVDL	551
Pma1	639	LQEKGHIVAMTGDGVNDAPALKRADIGIAMGKGGTEVAKESSDMLLT	686
PacL	649	LQRQGEFVAMTGDGVNDAPALKQANIGVAMGITGTDVSKEASDMVLL	696

E. Putative Metal-Binding Motif

CtaA	20	VEGMKCAGCVAAVERRLQQTAGVEAVSVNLITR	52
MenkesA	14	VEGMTCNSCVWTIEQQIGKVNGVHHIKVSLEEK	46
MenkesB	177	VEGMTCHSCTSTIEGKIGKLQGVQRIKVSLDNQ	209
MenkesC	283	IDGMHCKSCVSNIESTLSALQYVSSIVVSLENR	315
MenkesD	383	IDGMTCNSCVQSIEGVISKKPGVKSIRVSLANS	415
MenkesE	494	VTGMTCASCVANIERNLRREEGIYSILVALMAG	526
MenkesF	570	VRGMTCASCVHKIESSLTKHRGILYCSVALATN	602
CopA	12	ITGMTCANCSARIEKELNEQPGVMSATVNLATE	44
PacS	9	LRGMGCAACAGRIEALIQALPGVQECSVNFGAE	41
CadA	18	VQGFTCANCAGKFEKNVKKIPGVQDAKVNFGAS	50

FIG. 3. Amino acid sequence alignments of the predicted P-type ATPase CtaA with the conserved domains of several bacterial P-type ATPases and the human Menkes disease gene product. PacS and PacL (8), CopA, CopB (21), CadA (22), KdpB (6), and Pma1 (9) sequences have been published. (*A*) Phosphatase region. (*B*) Ion transduction region. (*C*) Phosphorylation site. (*D*) Hinge region and ATP-binding domain. (*E*) Putative metal-binding motifs and Menkes A-F Cu^{2+}-binding motifs in order (23–25). Amino acids are shown in boldface type at positions where they are identical in more than 50% of the sequences compared [by CLUSTAL V program (31)]. Asterisk (*) indicates the conserved aspartate residue that is the site of phosphorylation. For alignment purposes, a gap (-) was introduced in the sequences when needed.

in removing the phosphate group from the phosphorylation site (shown in Fig. 3*C*). The presumed "ion transduction" region (Fig. 3*B*) includes a proline residue (Pro^{433} in the *Synechococcus* CtaA sequence) that is conserved in all known P-type ATPases. It appears in a presumed membrane-spanning helical region and may participate in the conformational change responsible for opening and closing the transport channel (1–4). For the Menkes sequence (23–25) and four of the bacterial examples (8, 21, 22) shown, this proline residue is between cysteines that are thought to provide metal coordination (4, 21). The cysteines are not found in the KdpB K^+-ATPase sequence (6), nor in the other two cyanobacterial ATPase sequences, PacL and Pma1 (8, 9). The ion transduction region is thought to span the membrane and to constitute an essential part of the cation transduction channel and specificity determinant (4, 21). Note the higher degree of similarity among CtaA, PacS, the Menkes ATPase, CopA, and CopB in this region. Seven residues further in the sequence, another highly conserved proline occurs in this group of ATPases. Forty-four residues after the conserved proline in the membrane region is an absolutely conserved aspartate residue (Fig. 3*C*; Asp^{476} in the *Synechococcus* CtaA sequence). This is the amino acid that is phosphorylated during the ATPase/transport reaction cycle. The phosphorylation site includes, in addition to the aspartate residue, a region completely conserved for seven of nine residues in the nine examples shown (eight bacterial ATPases with different cation specificities plus the human Menkes ATPase).

Fig. 3*D* shows the alignment of a region that was previously referred to as the "hinge region" but later proposed to be an ATP-binding domain with a protein kinase activity (1–3, 5). In sum, the alignments shown in Fig. 3 *A–D* place the *Synechococcus* ATPase CtaA within the family of cation-translocating P-type ATPases from bacterial and animal sources.

Fig. 3*E* shows the alignment of a hypothesized "metal-binding motif" region shared by Cu^{2+} and Cd^{2+} P-type ATPases (4, 8). The *Synechococcus* CtaA sequence is about equally similar to that of the fifth human Menkes motif and the *Enterococcus* CopA sequence in this region (Fig. 3*E*; ref. 4).

Relationship of the CtaA ATPase to Other P-Type Cu^{2+}-ATPases. The sequence alignment trees in Fig. 4 suggest the placement of the CtaA ATPase among related proteins. However they mostly provide a basis for direct experimental testing. The amino acid comparison of the entire CtaA sequence with its closest homologs in the protein sequence libraries (Fig. 4*A*) suggests that CtaA may be a Cu^{2+}-uptake ATPase, most similar to CopA of *Enterococcus hirae* (21, 26). Disruption of the *copA* gene leads to a copper requirement for growth and disruption of the linked *copB* gene leads to greater copper sensitivity, leading to the current hypothesis that CopA is an uptake ATPase and CopB an efflux ATPase (21, 26). However, no transport data or intracellular copper measurements are available for *E. hirae*. Disruption of CopA also leads to higher resistance to Ag^+ cations than shown by wild-type cells, as if the CopA uptake ATPase shares a substrate specificity for Cu^{2+} and Ag^+. However, in our experiments *Synechococcus* wild-type and mutant K10 cells were equally sensitive to Ag^+ (data not shown).

Alignments of the entire P-type ATPase sequences (Fig. 4*A*) places CtaA closest to *Synechococcus* PacS (perhaps because of shared cellular origin) and *Enterococcus* CopA (perhaps because of shared cation specificity). The other two cyanobacterial P-type ATPases, PacL and Pma1, group together on a distant branch that includes the rabbit Ca^{2+}-ATPase.

The conservation of all essential motifs of P-type ATPases (Fig. 3) in CtaA leaves little doubt that the gene determines a P-type ATPase, but does not establish substrate specificity. The putative metal-binding motif of CtaA fits within the branch of the tree (Fig. 4*B*) ascribed to Cu^{2+}-binding motifs (4), along with the *Enterococcus* CopA sequence and those for human ATPases from Menkes syndrome and Wilson disease (27). These human hereditary diseases result from defective Cu^{2+} transport. Menkes syndrome is primarily related to blockage of Cu^{2+} uptake across the intestinal mucosal lining. Wilson disease is related to inability to discharge Cu^{2+} from the liver into blood circulation and bile. The other cyanobacterial metal-binding motif (from the PacS sequence of *Synechococcus* 7942) fits in another branch that consists otherwise of Cd^{2+}-efflux ATPases (Fig. 4*B*). However, disruption of the *pacS* gene leads to Cu^{2+} hypersensitivity (8), as if it were a Cu^{2+}-efflux ATPase. Cu^{2+} uptake measurements with still another cyanobacterium, *Nostoc calcicola*, were earlier interpreted as involving an efflux mechanism for Cu^{2+} resistance (28). For all metal-binding motifs in Fig. 4*B*, there are only sequences and computer

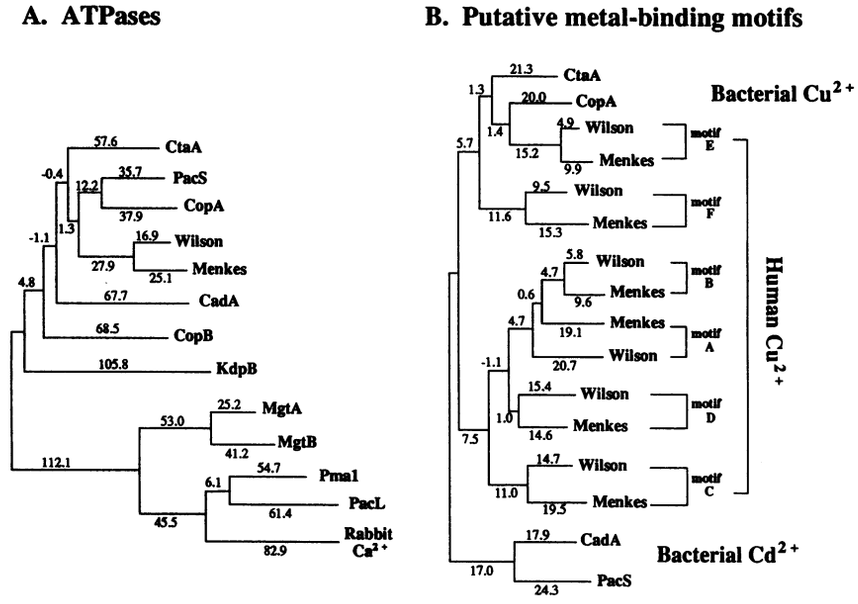

FIG. 4. Trees of sequence similarity relationships of the P-type ATPases. Tree of alignment of overall P-type ATPase sequences (*A*) and tree of alignment of putative metal-binding motifs (*B*) were produced by using the programs of Feng and Doolittle (17). The branch lengths are in arbitrary units, calculated from a scoring algorithm using both identities and close similarities between amino acids. The distances are considered to reflect actual evolutionary distances (17).

modeling. Only for the periplasmic Hg^{2+}-binding protein with a homologous metal-binding motif (not shown in Fig. 4*B*; ref. 4) are there experiments that show both the need for the conserved cysteines (29) and a structure based on NMR analysis (30).

The similarity between CtaA and the two human ATPases for Menkes syndrome and Wilson disease (Figs. 3 and 4) suggests that the cyanobacterial CtaA system will provide an experimentally accessible model for studies of structure–function relationships in the human gene products that also have been identified only from cDNA sequences and for which direct biochemical data are missing.

We thank M. Geisler, J. F. B. Mercer, J. I. Rood, S. Silver, and M. Solioz for helpful discussions and exchanges of unpublished results. We thank L. A. Scappino for technical assistance and K. G. Black for critical reading of the manuscript. This work was supported in part by a grant from the Human Frontiers of Science Program to R.H. and G.A. L.T.P. was a predoctoral trainee in Molecular Biophysics (National Institutes of Health Grant GM08528).

1. Pedersen, P. L. & Carafoli, E. (1987) *Trends Biochem. Sci.* **12**, 146–150.
2. Pedersen, P. L. & Carafoli, E. (1987) *Trends Biochem. Sci.* **12**, 186–189.
3. Scarpa, A., Carafoli, E. & Papa, S., eds. (1992) *Ann. N.Y. Acad. Sci.* **671**, 1–511.
4. Silver, S., Nucifora, G. & Phung, L. T. (1993) *Mol. Microbiol.* **10**, 7–12.
5. Serrano, R. (1988) *Biochim. Biophys. Acta* **947**, 1–28.
6. Hesse, J. E., Wieczorek, L., Altendorf, K., Reicin, A. S., Dorus, E. & Epstein, W. (1984) *Proc. Natl. Acad. Sci. USA* **81**, 4746–4750.
7. Altendorf, K., Siebers, A. & Epstein, W. (1992) *Ann. N.Y. Acad. Sci.* **671**, 228–243.
8. Kanamaru, K., Kashiwagi, S. & Mizuno, T. (1993) *FEBS Lett.* **330**, 99–104.
9. Geisler, M., Richter, J. & Schumann, J. (1993) *J. Mol. Biol.* **234**, 1284–1289.
10. Fresneau, C., Rivière, M.-E. & Arrio, B. (1993) *Arch. Biochem. Biophys.* **306**, 254–260.
11. Brown, N. L., Lee, B. T. O. & Silver, S. (1994) in *Metal Ions in Biological Systems*, eds. Sigel, H. & Sigel, A. (Dekker, New York), Vol. 30, pp. 405–434.
12. Herdman, M., Delaney, S. F. & Carr, N. G. (1973) *J. Gen. Microbiol.* **79**, 233–237.
13. Sambrook, J., Fritsch, E. F. & Maniatis, T. (1989) *Molecular Cloning: A Laboratory Manual* (Cold Spring Harbor Lab. Press, Plainview, NY), 2nd Ed.
14. Brusslan, J. A. (1988) Ph.D. thesis (University of Chicago, Chicago).
15. Schaefer, M. R. & Golden, S. S. (1989) *J. Bacteriol.* **171**, 3973–3981.
16. Muramatsu, S. & Mizuno, T. (1989) *Nucleic Acids Res.* **17**, 3982.
17. Feng, D.-F. & Doolittle, R. F. (1990) *Methods Enzymol.* **183**, 375–387.
18. Cozens, A. L. & Walker, J. E. (1987) *J. Mol. Biol.* **194**, 359–383.
19. Katz, M. E., Wright, C. L., Gartside, T. S., Cheetham, B. F., Doidge, C. V., Moses, E. K. & Rood, J. I. (1994) *J. Bacteriol.* **176**, 2663–2669.
20. Golden, S. S., Nalty, M. S. & Cho, D.-S. C. (1989) *J. Bacteriol.* **171**, 24–29.
21. Odermatt, A., Suter, H., Krapf, R. & Solioz, M. (1993) *J. Biol. Chem.* **268**, 12775–12779.
22. Nucifora, G., Chu, L., Misra, T. K. & Silver, S. (1989) *Proc. Natl. Acad. Sci. USA* **86**, 3544–3548.
23. Vulpe, C., Levinson, B., Whitney, S., Packman, S. & Gitschier, J. (1993) *Nat. Genet.* **3**, 7–13.
24. Mercer, J. F. B., Livingston, J., Hall, B., Paynter, J. A., Begy, C., Chandrasekharappa, S., Lockhart, P., Grimes, A., Bhave, M., Siemieniak, D. & Glover, T. W. (1993) *Nat. Genet.* **3**, 20–25.
25. Chelly, J., Tümer, Z., Tonnesen, T., Petterson, A., Ishikawa-Brush, Y., Tommerup, N., Horn, N. & Monaco, A. P. (1993) *Nat. Genet.* **3**, 14–19.
26. Odermatt, A., Suter, H., Krapf, R. & Solioz, M. (1992) *Ann. N.Y. Acad. Sci.* **671**, 484–486.
27. Bull, P. C., Thomas, G. R., Rommens, J. M., Forbes, J. R. & Cox, D. W. (1993) *Nat. Genet.* **5**, 327–337.
28. Verma, S. K. & Singh, H. N. (1991) *FEMS Microbiol. Lett.* **84**, 291–294.
29. Sahlman, L. & Skarfstad, E. G. (1993) *Biochem. Biophys. Res. Commun.* **196**, 583–588.
30. Eriksson, P.-O. & Sahlman, L. (1993) *J. Biomol. Nuclear Magn. Reson.* **3**, 613–626.
31. Higgins, D. G., Bleasby, A. J. & Fuchs, R. (1992) *Comput. Appl. Biosci.* **8**, 189–191.